

# Calibration of the two microphone transfer function method to measure acoustical impedance in a wide frequency range

**R. Boonen, P. Sas**

K.U.Leuven, Department of Mechanical Engineering,  
Celestijnenlaan 300 B, B-3001, Heverlee, Belgium  
e-mail: [rene.boonen@mech.kuleuven.ac.be](mailto:rene.boonen@mech.kuleuven.ac.be)

## Abstract

The acoustical impedance of a component is one of its most important characteristics. It is needed when acoustical simulations using lumped elements or electrical analog circuits are carried out. The calibration procedure for the two microphone transfer function method described in ISO 10534-2 is not sufficiently accurate in most cases.

In this paper, a new calibration method for the two microphone transfer function method has been proposed such that acoustical impedances can be measured with high accuracy over a wide frequency range. In this method, the estimation of the speed of sound has been eliminated. Next, in the calibration of the sensor mismatch, the deviation in sensor position after interchanging the pressure sensors has been taken into account. Finally, a recursive procedure has been proposed to refine the microphone position calibration. This refinement can be continued until the required calibration accuracy has been obtained.

## 1 Introduction

In acoustic applications, such as silencers, resonators, absorbant materials, horns, etc . . . , acoustic characterization is necessary to successfully design the acoustical system. Such systems are likely simulated using lumped element models or electrical analog circuits. The acoustical impedance of a component is one of the most important characteristics of the component. Therefore, accurate acoustical impedance measurement methods are required.

Dalmont [1] presents in his paper an overview of several techniques for acoustical impedance measurement.

The most straight forward technique is using a pressure and a volume velocity sensor [1], whereby the impedance is calculated directly from its ratio. The direct measurement of the volume velocity can be carried out using for example a hot wire anemometer. Another approach is using an excitation source with a known volume velocity.

A common acoustical impedance measurement technique is the standing wave ratio (SWR) method (the classical Kundt duct). This method is described in the ISO-10534-1 standard. The ends of the Kundt duct are closed by an excitation source at one end and the unknown impedance at the other end. The source generates a sinusoidal signal which results in a standing wave pattern in the duct. Along the axis of the duct, a microphone is moved. The minimum and maximum pressure amplitude of the standing wave and the location where the minimum and maximum amplitude occurs are determined. From these data, the reflection coefficient and the acoustical impedance are calculated.

Other methods are based to connect known impedances to the impedance to be measured, in order to characterize the unknown impedance. These methods are mostly used to determine the internal acoustical impedance of a source [2, 3, 4]. To the impedance to be measured, known acoustical loads are connected and the response to a source will be measured. A set of equations results, from which the unknown impedance

can be determined. However, the equation set is often ill conditioned and its results can deviate strongly from reality.

A widely used method is the "two microphone transfer function method", which is described in ISO-10534-2. This method uses the transfer function measured between two pressure sensors at two distinct positions in the measurement wave guide to determine the acoustical impedance attached at one side of the wave guide. This method is discussed in detail in the next section.

When the acoustical impedance is needed over a wide frequency band, for example from 10Hz to 10kHz, all the impedance measurement methods described above shows limitations. In this paper, a new calibration method has been proposed such that acoustical impedances can be measured with high accuracy over a wide frequency range. In this method, the estimation of the speed of sound has been eliminated. Next, in the calibration of the sensor mismatch, the deviation in sensor position after interchanging the pressure sensors has been taken into account. Finally, a recursive procedure has been proposed to refine the microphone position calibration. This refinement can be continued until the required calibration accuracy has been obtained.

## 2 The two microphone transfer function method

### 2.1 Principle of the method

In this section, the two microphone transferfunction method according to ISO 10534-2 is discussed. Figure 1 presents the set-up for acoustical impedance measurement. The set-up consists of a straight duct which is the measurement acoustic wave guide. At the right end, an excitation source, for example a loudspeaker is connected. At the left end, the impedance to be measured is connected. This impedance includes everything present at the right side of the reference section. The reference section isn't necessarily a physical connection point. It is a mathematical position. The acoustical impedance can be re-calculated at a different reference section, without re-measuring the transfer functions. Two microphones at two distinct positions  $x_1$  and  $x_2$  measure the sound pressure inside the duct. From the transfer function between the two microphones, the reflection coefficient and consequently, the unknown connected impedance will be determined.

Figure 2 shows the electrical analog circuit [6] of the set-up presented in figure 1. The three transmission lines  $T_1$ ,  $T_2$  and  $T_3$  represent the measurement wave guide. The voltages at  $x_1$  and  $x_2$ , representing the pressures at these locations, will be used to determine the reflection coefficient. The current source  $I_g$ , representing a volume velocity, with internal source impedance  $Z_g$  excites the system. The impedance  $Z_l$  to be measured situates at right side of the reference section.

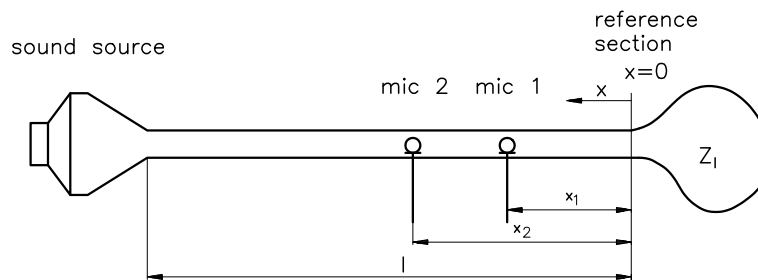


Figure 1: Wave guide with an unknown acoustical impedance  $Z_l$ .

In the frequency domain, the wave pattern in the wave guide is governed by the one-dimensional Helmholtz wave equation, which describes the pressure distribution along the wave guide. At each position  $x$ , the pressure in terms of the wave number  $k$  in the wave guide equals [7]:

$$p(x, k) = I_g \frac{Z_0 Z_g}{Z_0 + Z_g} \cdot \frac{e^{-jkl}}{1 - \Gamma_l \Gamma_g e^{-j2kl}} \cdot (e^{jkx} + \Gamma_l e^{-jkx}) \quad (1)$$

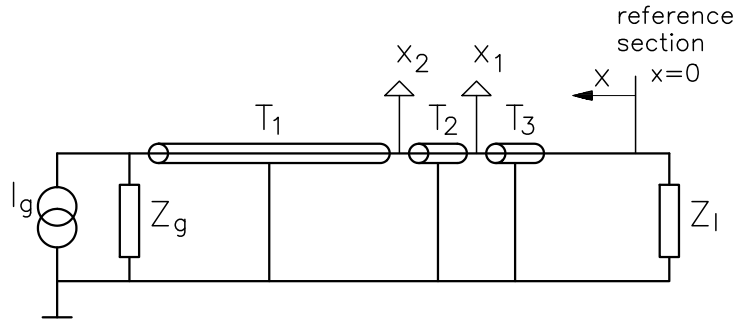


Figure 2: Electrical analog circuit of the set-up presented in figure 1.

wherein  $k$  is the wave number and  $l$  the distance between the exciting sound source and the reference section. Referring to the electrical analog circuit in figure 2, the source current  $I_g$  splits over the source internal impedance  $Z_g$  and the wave guide characteristic impedance  $Z_0$ . The current flowing through the wave guide reflects alternately at the load impedance  $Z_l$  with a reflection coefficient  $\Gamma_l$  and at the source impedance  $Z_g$  with a reflection coefficient  $\Gamma_g$ . As  $\Gamma_l < 1$  and  $\Gamma_g < 1$ , the sum of the series of reflections is finite and equals the factor  $e^{-jkl}/(1 - \Gamma_l \Gamma_g e^{-j2kl})$ . The factor  $(e^{jkx} + \Gamma_l e^{-jkx})$  describes the pressure distribution in the duct in terms of position.

To measure the load impedance using the two microphone method, the transfer function  $T_{12}$  between the pressures at two distinct positions  $x_1$  and  $x_2$  is taken:

$$T_{12} = \frac{p(x_1, k)}{p(x_2, k)} = \frac{e^{jkx_1} + \Gamma_l e^{-jkx_1}}{e^{jkx_2} + \Gamma_l e^{-jkx_2}} \quad (2)$$

Notice that the source reflection coefficient drops out, the reflection coefficient at the load is the single unknown. Consequently, the choice of the source type is free.

Isolating the load reflection coefficient from equation (2) results in:

$$\Gamma_l = -\frac{e^{jkx_1} - T_{12} e^{jkx_2}}{e^{-jkx_1} - T_{12} e^{-jkx_2}} \quad (3)$$

Finally, the load impedance will be calculated using equation (3) [7]:

$$\begin{aligned} Z_l &= Z_0 \frac{1 + \Gamma_l}{1 - \Gamma_l} \\ &= jZ_0 \frac{\sin kx_1 - T_{12} \sin kx_2}{\cos kx_1 - T_{12} \cos kx_2} \end{aligned} \quad (4)$$

## 2.2 Calibration of the set-up according to ISO 10534-2

Equation (4) becomes inaccurate when the reflection coefficient  $\Gamma_l$  approaches unity. In this case, a small error in the reflection coefficient result in a large deviation of the obtained impedance. This situation occurs when the unknown impedance deviates largely from the characteristic impedance of the wave guide. Therefore, prior calibration of the set-up is necessary to obtain accurate results.

The ISO 10534-2 standard demands the following calibration actions:

- The velocity of sound needs to be determined accurately using measurements of ambient temperature and atmospheric pressure.

- The distance between the pressure sensors need to be measured accurately.
- The mismatch between the amplitude and phase of the pressure sensors needs to be calibrated. In short, the procedure is to measure the transfer function  $T_{12}$  of the two pressures at position  $x_1$  and  $x_2$ , then interchange the two pressure sensors from location  $x_1$  to  $x_2$  and from  $x_2$  to  $x_1$  respectively, measure the transfer function  $T_{21}$  and calculate the calibration factor  $\delta$  such that:

$$\delta^2 T_{12} T_{21} = 1 + 0j \quad (5)$$

This calibration factor  $\delta$  is complex and frequency dependent.

In order to illustrate the quality of the ISO calibration procedure, graphs are presented based on theoretical calculations wherein realistic data for such set-up are used.

Suppose the wave guide has a diameter of 36 mm, the characteristic impedance will be  $Z_0 = 400 \text{ k}\Omega$  ( $1 \Omega = 1 \text{ Pa s/m}^3$ ). The distance between the closest pressure sensor and the reference section is  $x_1 = 0.2 \text{ m}$  and between the farthest pressure sensor and the reference section  $x_2 = 0.5 \text{ m}$ . When the impedance measurement range is limited to 120 dB (ref.  $Z_0$ ), i.e. 60 dB above and below  $Z_0$ , the closed duct ("infinite") impedance  $Z_l$  will be limited to  $1000Z_0$ .

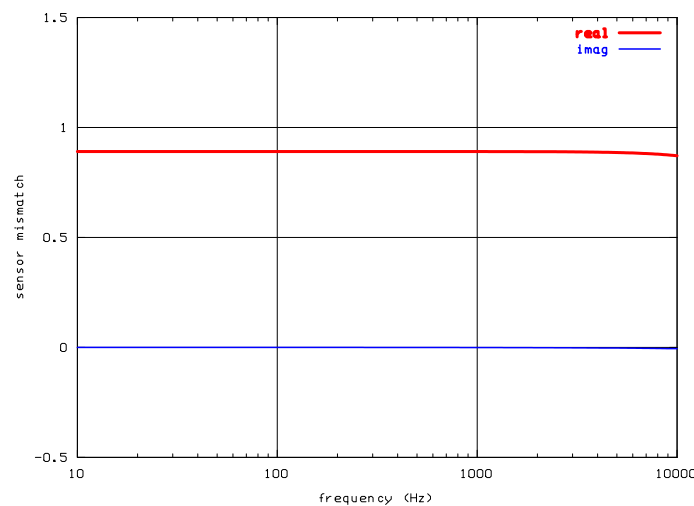


Figure 3: Mismatch between pressure sensor 1 and sensor 2.

The sensor sensitivities (for example piezo-electric sensors) behave most likely as second order spring-mass systems. The relation between the sensor output voltages  $u_i$  ( $i = \text{sensor number } 1, 2$ ) and input pressures  $p_i$  ( $i = 1, 2$ ) are in this case:

$$u_i = K_i \frac{\omega_i^2}{\omega_i^2 - \omega^2 + j \xi_i \omega_i \omega} p_i \quad (6)$$

It is supposed that the first sensor has an amplification  $K_1 = 0.98$ , a resonance frequency of  $\omega_1 = 2\pi 42000/\text{s}$  and a damping coefficient of  $\xi_1 = 0.05$ , and the second sensor  $K_2 = 1.10$ ,  $\omega_2 = 2\pi 36000/\text{s}$  and  $\xi_2 = 0.02$ . Figure 3 presents the resulting sensor mismatch in real and imaginary parts.

The uncorrected transfer function between the output voltages of the two pressure sensors is presented in figure 4.

When the inverse transfer function has to be measured, the interchanged pressure sensors can not be mounted at the exact same locations. Suppose that the new locations deviate 0.2 mm from the original locations, then

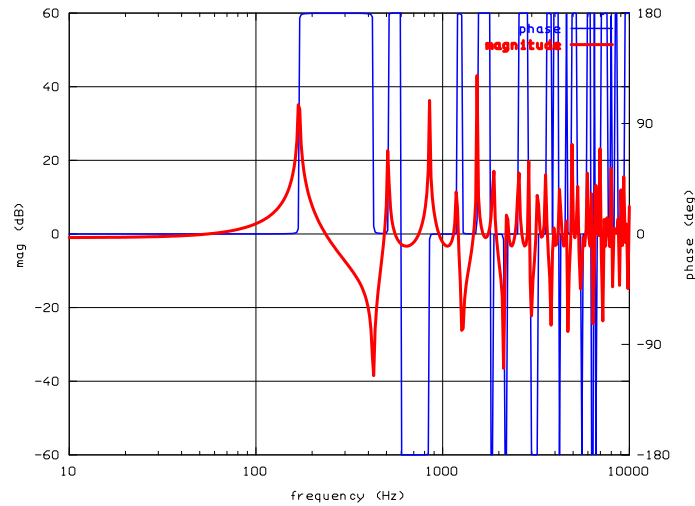


Figure 4: Transfer function between the pressure sensor signal  $u_1$  and the sensor signal  $u_2$ .

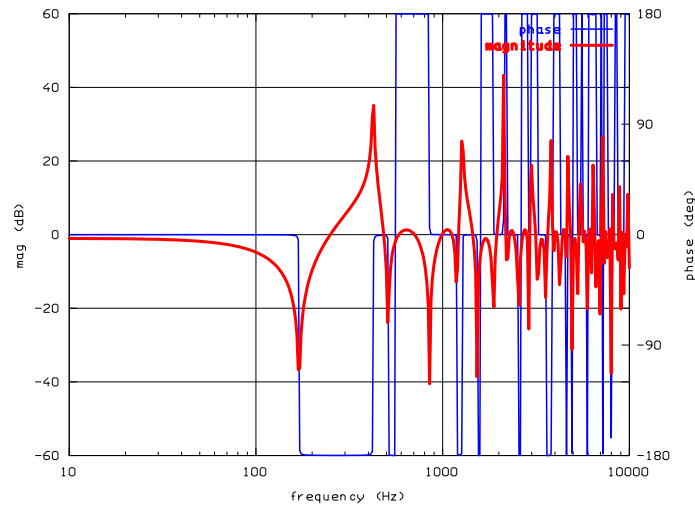


Figure 5: Reverse transfer function between the pressure sensor signal  $u_2$  and the sensor signal  $u_1$ .

the new locations will be  $X_1 = 0.2002$  m and  $X_2 = 0.4998$  m in stead of  $x_1$  en  $x_2$  respectively. The inverse transfer function at the new positions is presented in figure 5.

Now, the calibration method described in the ISO 10534-2 standard is applied. The resulting calibration factor  $\delta$  times the sensor mismatch is presented in figure 6. This product should equal  $1 + 0j$ . In the lower frequency range, the calibration has been successful. However, in the higher frequency range, starting from 150 Hz, the calibration is erroneous and even worse than the uncalibrated situation. The resulting impedance is presented in figure 7. This should be a straight line at 60 dB, but due to the erroneous calibration, large deviations results. In this case, the measurement range wherein the unknown impedance can be reliably measured is limited to 40 dB around  $Z_0$  until 400 Hz. Above 400 Hz, reliable impedance measurements are not possible.

Therefore, it will be necessary to calibrate the pressure sensor positions accurately for both transfer function  $T_{12}$  and  $T_{21}$ , and use these positions to calibrate the sensor mismatch.

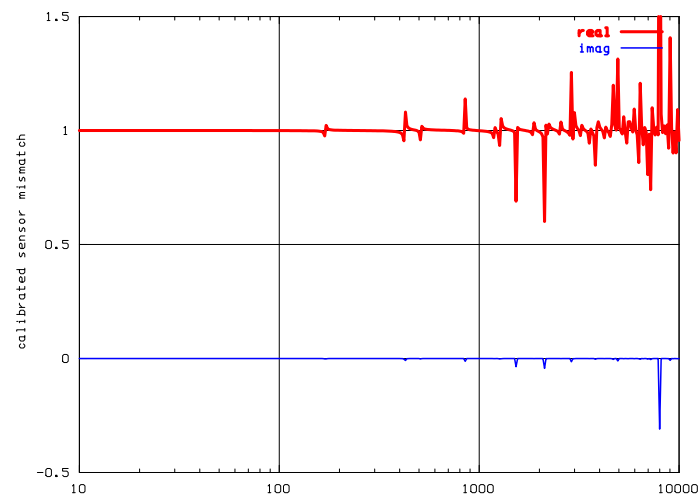


Figure 6: Calibration result of the pressure sensors according to ISO 10534-2.

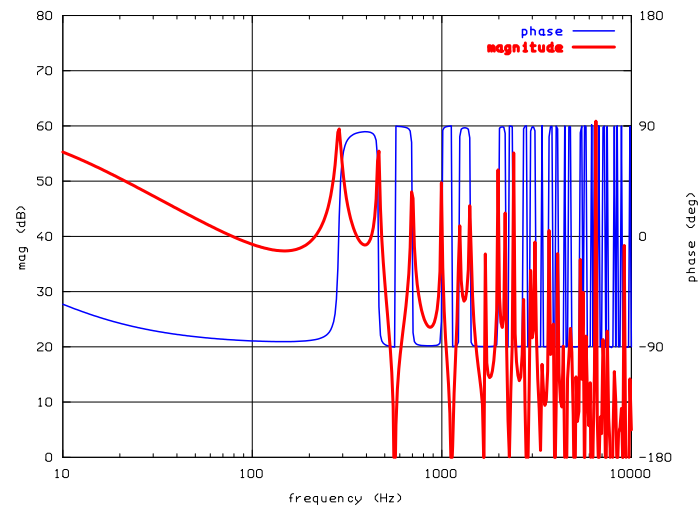


Figure 7: Resulting closed duct end impedance using the calibration data displayed in figure 6.

### 3 Improved calibration of the set-up

In this paper, an improved calibration procedure is proposed. The calibration is carried out with the wave guide closed at the reference section, so a hard wall reflection will occur.

The improved method introduces the following actions:

1. The speed of sound will be eliminated by replacing the variable  $kx$  by  $\omega t$ . This action eliminates the calibration of the speed of sound. Consequently, the temperature and ambient pressure measurements are superfluous.
2. The wave guide is closed at the reference section. The resulting acoustic impedance will be evaluated at specific frequencies to calculate the correct distances of the pressure sensors to the reference section. These distances are represented by the time the acoustic wave needs to travel from the respective sensor positions to the reference section.
3. The calibration of the sensor mismatch has been carried out whereby the sensor position deviation, caused by interchanging the sensors, is taken into account.

The result is an iterative procedure, which can be stopped when the required accuracy is reached.

### 3.1 Elimination of the speed of sound

The speed of sound is eliminated by replacing  $kx_i$  by  $\omega t_i$ , ( $i = 1, 2$ ), in expression (2), wherein  $t_1$  and  $t_2$  are the times the wave needs to travel from the positions  $x_1$  and  $x_2$  to the reference section respectively.

These traveling times  $t_1$  and  $t_2$  are estimated from the transfer function  $T_{12}$  (figure 4) where they correspond with the first pole for the farthest microphone and the first zero for the nearest microphone. The pole and the zero correspond to the first node of the pressure distribution of the standing wave appearing at the positions  $x_1$  and  $x_2$  respectively. These traveling times  $t_1$  and  $t_2$  equals:

$$t_1 = \frac{1}{4f_1} \quad \text{and} \quad t_2 = \frac{1}{4f_2} \quad (7)$$

wherein the frequencies  $f_1$  and  $f_2$  are associated to the frequencies determined by the quarter wavelength between the reference section and the positions  $x_1$  and  $x_2$  respectively.

In the same way, the travelling times  $T_1$  and  $T_2$  after exchanging the microphones are estimated from the transfer function  $T_{21}$  (figure 5), where  $F_1$  is the frequency corresponding to the first zero for the farthest microphone and  $F_2$  to the first pole for the nearest microphone.

$$T_1 = \frac{1}{4F_1} \quad \text{and} \quad T_2 = \frac{1}{4F_2} \quad (8)$$

### 3.2 Calibration of the sensor mismatch

Once  $t_1$ ,  $t_2$ ,  $T_1$  and  $T_2$  are determined, the sensor mismatch can be calibrated. The relation between the pressure transfer functions  $T_{p12} = p(x_1)/p(x_2)$  and  $T_{p21} = p(x_2)/p(x_1)$  is:

$$T_{p12} T_{p21} = 1 \quad (9)$$

These pressure transfer functions are measured using microphones. So, the transfer functions between microphone output signals  $u(x_1)$  and  $u(x_2)$  is  $T_{u12} = u(x_1)/u(x_2)$  and  $T_{u21} = u(x_2)/u(x_1)$ , which deviate from the pressures  $p(x_1)$  and  $p(x_2)$  in amplitude and phase by a factor  $\delta$ , i.e.

$$\delta^2 T_{u12} T_{u21} = 1 + 0j \quad (10)$$

However, the interchanged sensors cannot be mounted exactly at the positions  $x_1$  and  $x_2$  again. Consequently, the transfer function  $T_{u21} = u(x_2)/u(x_1)$  is not available. This transfer function  $T_{u21}$  needs to be calculated from the transfer function  $T_{U21} = u(X_2)/u(X_1)$ , which is measured at the positions  $X_1$  and  $X_2$ . These new positions deviate only slightly from the original positions.

To find the transfer function  $T_{u21}$ , the transfer function  $T_{U21}$  needs to be "shifted" as if it would be determined at the positions  $x_1$  and  $x_2$  instead of  $X_1$  and  $X_2$ . To find the way how to shift the transfer function, the acoustical impedance at a common reference section is considered.

The transfer function  $T_{p21}$  equals:

$$T_{p21} = \frac{Z_l \cos \omega t_2 + jZ_0 \sin \omega t_2}{Z_l \cos \omega t_1 + jZ_0 \sin \omega t_1} \quad (11)$$

In the same way, the transfer function  $T_{P21}$  between the pressures at the positions  $X_2$  and  $X_1$  equals:

$$T_{P21} = \frac{Z_l \cos \omega T_2 + jZ_0 \sin \omega T_2}{Z_l \cos \omega T_1 + jZ_0 \sin \omega T_1} \quad (12)$$

The reference section is identical in the two cases. Consequently, the acoustic impedance  $Z_l$  is equal in equation (11) and (12). Eliminating  $Z_l/(jZ_0)$  from equation (11) and (12) yields:

$$T_{p21} = \frac{\sin \omega (t_2 - T_2) - T_{p21} \sin \omega (t_2 - T_1)}{\sin \omega (t_1 - T_2) - T_{p21} \sin \omega (t_1 - T_1)} \quad (13)$$

With  $T_{p21} = T_{u21} \delta$  and  $T_{p21} = T_{U21} \delta$ , equation (13) becomes ultimately:

$$T_{u21} = \frac{1}{\delta} \left( \frac{\sin \omega (t_2 - T_2) - T_{U21} \delta \sin \omega (t_2 - T_1)}{\sin \omega (t_1 - T_2) - T_{U21} \delta \sin \omega (t_1 - T_1)} \right) \quad (14)$$

Introducing equation (14) in (10) and solving for  $\delta$  yields:

$$\delta = -\frac{1}{2} \left[ \left( \frac{\sin \omega (t_1 - T_1)}{T_{u12} \sin \omega (t_2 - T_1)} + \frac{\sin \omega (t_2 - T_2)}{T_{U21} \sin \omega (t_2 - T_1)} \right) \pm \sqrt{\left( \frac{\sin \omega (t_1 - T_1)}{T_{u12} \sin \omega (t_2 - T_1)} + \frac{\sin \omega (t_2 - T_2)}{T_{U21} \sin \omega (t_2 - T_1)} \right)^2 - 4 \frac{\sin \omega (t_2 - T_2)}{T_{u12} T_{U21} \sin \omega (t_2 - T_1)}} \right] \quad (15)$$

The correction factor  $\delta$  is complex and frequency dependent. The correct sign of the square root in  $\delta$  needs to be determined on physical basis. It can be selected by inspecting the plot of  $\delta$  in terms of frequency.

Finally, the unknown impedance will be determined using:

$$Z_l = jZ_0 \frac{\sin \omega t_1 - T_{u12} \delta \sin \omega t_2}{\cos \omega t_1 - T_{u12} \delta \cos \omega t_2} \quad (16)$$

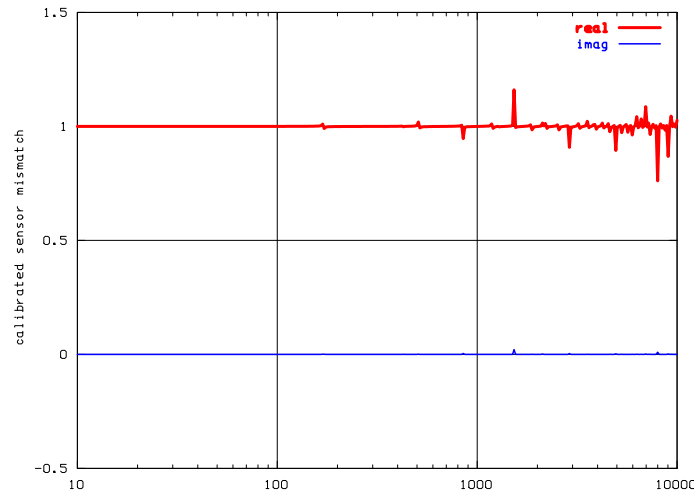


Figure 8: Calibration result of the pressure sensors using the travelling times between the sensor positions and the reference section, based on equations (7), (8) and (15).

Figure 8 shows the correction factor  $\delta$  obtained using this procedure. It is improved compared to figure 6. The resulting acoustical impedance of the closed duct is presented in figure 9. Now, the resulting impedance is higher than the impedance obtained with the ISO 10534-2-procedure (see figure 7). The range wherein the unknown impedance can be measured within 40 dB around  $Z_0$  is now expanded to 1 kHz. However, further refinement of the calibration is necessary if the frequency range needs to be expanded to 10 kHz.

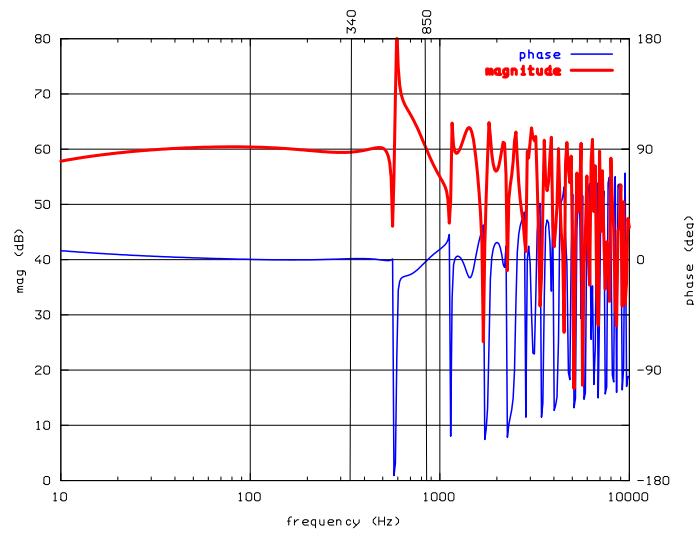


Figure 9: Resulting closed duct end impedance using the calibration data displayed in figure 8.

### 3.3 Refining the sensor position calibration

In most cases, the travelling times  $t_1$ ,  $t_2$ ,  $T_1$  and  $T_2$  are still not sufficiently accurate when determined from the equations (7) and (8). The impedance is extremely sensitive to errors in the travelling times. Therefore, the acoustical impedance of the closed duct itself will be used to refine these travelling times. The transfer functions or the reflection coefficient are not sufficiently sensitive to refine the travelling times.

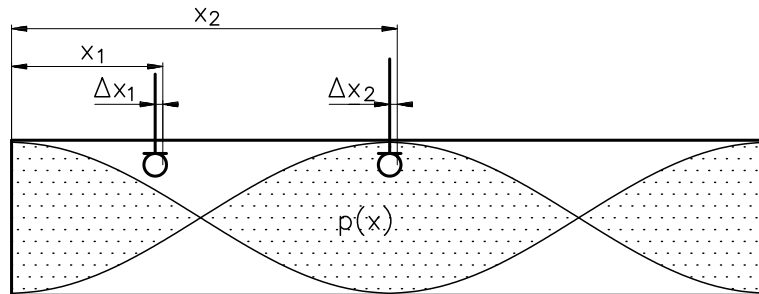


Figure 10: The situation wherein the travelling time  $t_1$  will be corrected.

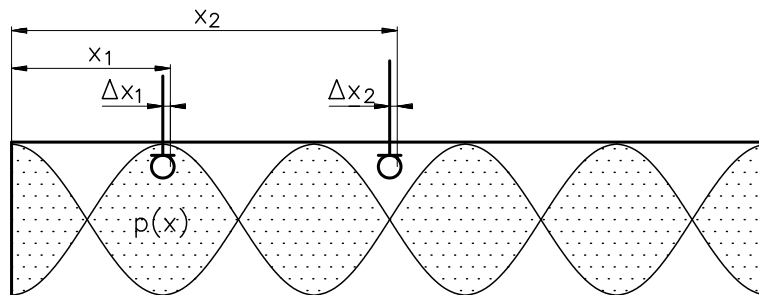


Figure 11: The situation wherein the travelling time  $t_2$  will be corrected.

The refining of the travelling times can be executed for each travelling time separately. Figures 10 and 11 present the situations wherein respectively the travelling times  $t_1$  and  $t_2$  will be corrected. When a pressure

maximum occurs at one of the microphone positions, the gradient of the pressure is zero and a small deviation of the microphone position does not affect the accuracy of the result. The other microphone position, where the gradient is generally not zero, determines fully the observed impedance. At the frequencies where this phenomenon occurs, the deviation of the microphone position can be accurately determined. In the case where the pressure maxima occurs at the two microphone positions simultaneously, this approach will fail. So, at the design stage of the measurement wave guide, the positions of the microphones and the reference section may not be equidistant.

The correction of the travelling time  $\tau_1$  will be determined when a half wave length stands at position  $x_2$  (see figure 10):

$$\frac{n}{2}\lambda = x_2 + \Delta x_2 \approx x_2 \quad n = 1, 2, 3, \dots \quad (17)$$

where  $\Delta x_2$  is the deviation to  $x_2$  and is very small. The frequency where this situation occurs is:

$$f_2 = \frac{n}{2t_2} \quad n = 1, 2, 3, \dots \quad (18)$$

In the same way, the frequency where the correction of the travelling time  $\tau_2$  will be determined will be:

$$f_1 = \frac{n}{2t_1} \quad n = 1, 2, 3, \dots \quad (19)$$

At these distinct frequencies, the distance between the two microphones is virtually correct, because a small deviation of the position of the microphone at the pressure maximum does not affect the calibration accuracy. As a result, a load impedance appears at the reference section which is composed of the hard wall impedance and a short piece wave guide with length  $\Delta x$ . ( $\Delta x_1$  at frequency  $f_2$  and  $\Delta x_2$  at frequency  $f_1$ ) The impedance in this situation is equivalent with the circuit presented in figure 12. As the impedance of a hard wall approaches

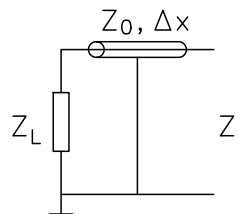


Figure 12: Equivalent circuit to determine the impedance  $Z_l$  of a piece wave guide with a length  $\Delta x$  connected to the hard wall impedance  $Z_L$ .

infinity, the impedance found at the reference section at angle frequency  $\omega_2 = 2\pi f_2$  will be:

$$Z_l = \frac{Z_0}{j} \cot \omega_2 \tau_1 \quad (20)$$

When evaluating the impedance obtained from equation (20) at  $f_2$  for  $n = 1$ , the correction on the travelling time  $t_1$  will be:

$$\tau_1 = \frac{t_2}{\pi} \arctan \frac{Z_0}{jZ_l} \quad (21)$$

In the same way, the correction on the travelling time  $t_2$  will be:

$$\tau_2 = \frac{t_1}{\pi} \arctan \frac{Z_0}{jZ_l} \quad (22)$$

This correction of the travelling times can be repeated until the required accuracy has been obtained.

In the same way, the travelling times  $T_1$  and  $T_2$  will be corrected.

### 3.4 Calibration procedure

The procedure is executed as follows:

1. The travelling times  $t_1$  and  $t_2$  will be estimated from the first pole and zero of the measured transfer function  $T_{u12}$  and  $T_1$  and  $T_2$  from the first zero and pole of the measured transfer function  $T_{U21}$  using equations (7) and (8).
2. The calibration factor  $\delta$  will then be estimated from the transfer functions  $T_{u12}$  and  $T_{U21}$  using equation (15).
3. Then the refining proces starts with above data as input. Subsequently, the correction on  $t_1$  and  $t_2$  is calculated using equations (21) and (22) respectively. Also the correction on  $T_1$  and  $T_2$  is calculated using the same equations. Then the transfer functions  $T_{u12}$  and  $T_{U21}$  are re-calibrated using equation (15). This proces is repeated until the travelling times and the sensor mismatch calibration have reached the required accuracy.

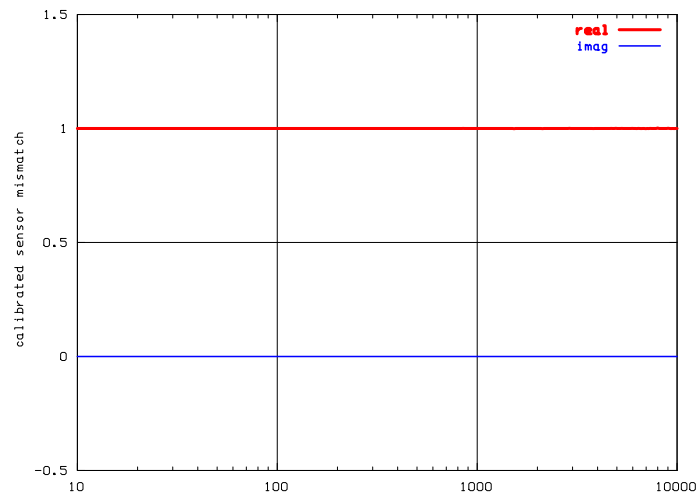


Figure 13: Calibration result of the pressure sensors after refining the sensor distances.

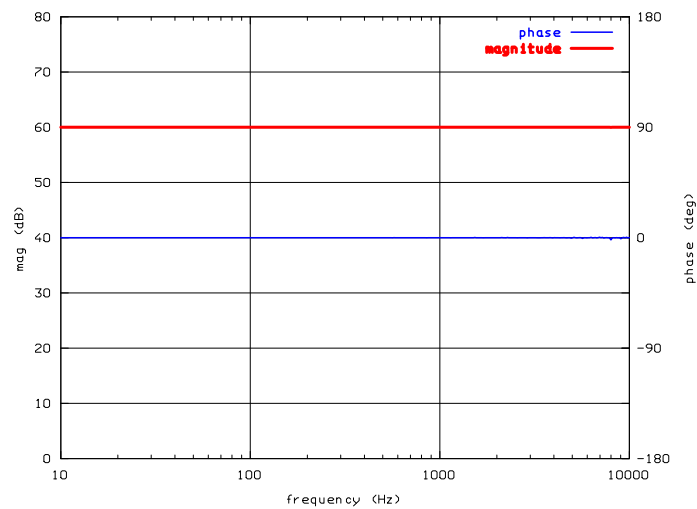


Figure 14: Resulting closed duct end impedance using the calibration data displayed in figure 13.

Figure 13 shows the calibration result after applying the procedure, where the travelling times have been converged within  $10^{-6}$ . The resulting impedance is displayed in figure 14. Now, it is possible to measure a load impedance within 60 dB range around  $Z_0$  over the whole frequency range from 10 Hz to 10 kHz.

The next step will be the experimental verification of this calibration procedure.

## 4 Conclusion

This theoretical investigation about the calibration of the two microphone transfer function method leads to the following conclusions:

- The accuracy of the calibration method described in the ISO-10534-2 standard is not sufficient for impedance measurements in most applications.
- The improved method has eliminated the speed of sound and replaced it by the travelling times the waves need to travel from the microphone position to the reference section. The measurements of ambient temperature and atmospheric pressure have become superfluous.
- The deviations in position which occur by interchanging the pressure sensors when calibrating the sensor mismatch has been taken into account.
- A refinement procedure for accurate sensor position determination has been proposed. This procedure allows to iterate the sensor positions until the required accuracy has been obtained.

As result, acoustical impedance can be measured accurately in a wide frequency range.

## References

- [1] J.-P. Dalmont, *Acoustic impedance measurement, part I, A review*, J. Sound and Vibration, Vol. 243, No. 3 (2001), pp. 441-459.
- [2] M. G. Prasad, *A four load method for evaluation of acoustical source on a duct*, J. Sound and Vibration, Vol. 114, No. 2 (1987), pp. 347-356.
- [3] L. Desmons, J. Hardy and Y. Auregan, *Determination of the acoustical source characteristics of an internal combustion engine by using several calibrated loads*, J. Sound and Vibration, Vol. 179, No. 5 (1995), pp. 869-878.
- [4] H. Bodén, *On multi-load methods for determination of the source data of acoustic one-port sources*, J. Sound and Vibration, Vol. 180, No. 5 (1995), pp. 725-743.
- [5] ISO 10534-2, *Determination of sound absorption coefficient and impedance in impedance tubes*, International Organisation for Standardization, Case postale 56, CH-1211 Genève 20, (1998).
- [6] L. L. Beranek, *Acoustics*, Mc Graw-Hill, (1954)
- [7] H. P. Neff, Jr, *Basic Electromagnetic Fields*, Harper & Row, (1987)
- [8] R. Boonen, P. Sas, *Determination of the acoustical impedance of an internal combustion engine exhaust in Proceedings of The ISMA2002 Conference*, Leuven, Belgium, (2002), vol V, pp. 1939-1946.